Self-oscillations at photoinduced impurity breakdown in GaAs

M. Kozhevnikov, B. M. Ashkinadze, E. Cohen, and Arza Ron
Solid State Institute, Technion–Israel Institute of Technology, Haifa 32000, Israel
(Received 17 February 1995)

The effects of microwave (MW) irradiation on photoexcited free and donor-bound electrons are studied in semi-insulating, bulk GaAs in the temperature range of 2–20 K. The main observations are as follows: an abrupt increase in the photoinduced microwave absorption (PMA), a concurrent decrease of the donor-acceptor pair photoluminescence and self-oscillations in the PMA when the incident MW power exceeds a threshold value. The PMA self-oscillation frequency varies with photoexcitation intensity and incident MW power in the range of 0.5–3 kHz. These nonlinear phenomena are observed under spatially uniform MW irradiation and photoexcitation, without any electrical contacts. A model is developed for the dependence of the free and donor-bound electron densities on the microwave power and photoexcitation intensity under the conditions of donor impact ionization (breakdown) by the MW heated free electrons. A linear dependence of the electron temperature on the free-electron density is assumed. The self-oscillation frequency is determined by the remote donor-acceptor recombination rate. The model-calculated steady state and self-oscillations of the free-electron density agree well with the observed PMA behavior. It is thus shown that spatially uniform self-oscillations are an intrinsic property of the photoinduced impurity breakdown.

I. INTRODUCTION

In the early 1980s a renewed interest arose in hot-electron phenomena in semiconductors. In particular, electric current instabilities, self-oscillations, and chaos were considered as results of the complex behavior of a nonlinear dynamic system that is easily affected by an applied electric field and by photoexcitation.[1–6] At low temperatures these instabilities usually occur when a sharp transition from a nonconducting to a conducting state is induced by the applied electric field. The basic physical mechanism governing these effects is the impact ionization of electrons (holes) bound to shallow impurities by free carriers that are heated by the electric field.[7–9] Similar breakdown phenomena were also observed in pure or compensated semiconductors under photoexcitation. In this case the donors (or acceptors) are ionized in the dark, and the photoexcitation leads to their neutralization and subsequently to impurity or excitation impact ionization.[10–12]

Regular and chaotic electric current self-oscillations, that are often observed at impurity breakdown, are associated with an *S*-shaped current-voltage characteristic [namely, with a negative differential conductivity (NDC)]. In the NDC region, current or electric-field distributions are unstable with respect to a fluctuation growth of current filaments or fields domains.[13] A motion of the current filaments (or field domains) or an external circuit will cause temporal instabilities of the electric current when a breakdown is induced by an applied, direct electric field.[4–6]

In several studies, microwave (MW) irradiation was used for charge-carrier heating instead of a dc electric field.[12,14–17] This contactless method allows the study of impurity breakdown under spatially homogeneous conditions that exclude both electric-field and electric current redistributions, and eliminates effects due to the external circuit. Growth of any carrier density fluctuations is also expected to be attenuated when the electric field varies at microwave frequency. Nevertheless, self-oscillations in the electron density were observed in photoexcited Ge, Si, and GaAs crystals, at $T < 10$ K, under the spatially homogeneous conditions of MW irradiation.[12,17]

Current and electric-field instabilities are commonly analyzed within the framework of the phenomenological impurity-breakdown model that assumes impact ionization of both the 1*s* and 2*s* neutral donor (or acceptor) levels by the heated free electrons. This model was introduced by Kastalskii[18] in order to explain the *S*-shaped current-voltage characteristic of compensated Ge at low temperatures. Schöll[4,6] used this model in order to describe the impurity-breakdown phenomenon as a nonequilibrium phase transition. He analyzed both stationary and dynamic current-voltage dependencies and showed that current instabilities become possible only if both spatial and temporal variations of the electrical field (dielectric relaxation) or the slow energy relaxation of hot carriers are taken into consideration. Recently, Quade *et al.*[19] carried out a Monte Carlo simulation of the microscopic breakdown model for the case of *p*-type Ge, and Kehrer, Quade, and Schöll[20] did the same for *n*-type GaAs. Their results demonstrated that the *S*-shaped, dc current-voltage behavior and the associated instabilities are predicted only if a two-level model is used (in contrast to a one-level donor model). However, these authors did not take into account some specific features of hot-electron processes at low temperatures. For example, the runaway of hot electrons (namely, an electron overheating[13]) and the increased screening of the electron scattering by ionized impurities as the breakdown occurs were not considered. These phenomena were believed to be essential in the earlier phenomenological models of im-

purity breakdown.[7–9,13,21] In these studies, impact ionization of only the 1*s* donor state was considered, and the *S*-shaped current-voltage curve was associated with various mechanisms leading to an increased mobility as the electron density increased under breakdown conditions. Therefore, though the two-level model is often used for the analysis of the nonlinear behavior and various instabilities of both the dark current and the photocurrent, as well as of the photoluminescence (PL) intensity dependence on the electric field,[5,6,11] a comprehensive microscopic theory is still unavailable. Moreover, there is no phenomenological model taking into account the recombination of nonequilibrium charge carriers and their overheating in analyzing instabilities under photoinduced breakdown conditions.

In this study we present an experimental investigation of the photoinduced breakdown of shallow donors in nominally undoped semi-insulating GaAs at low temperatures under spatially homogeneous MW irradiation conditions. The stationary and temporal dependence of the photoinduced MW absorption (PMA) and of the exciton and donor-acceptor pair photoluminescence (PL) on incident MW power and light excitation intensity as well as on temperature were studied. Abrupt variations of both PMA and PL intensities at a threshold MW power and self-oscillations in the PMA in a certain range of the MW power and photoexcitation intensity were observed. Experimental results are analyzed in terms of a phenomenological model for the spatially homogeneous photoinduced breakdown of shallow donors. Impact ionization of only the 1*s* donor level is considered, and the dependence of the electron temperature on the free-electron density is explicitly introduced. The steady-state and dynamic solutions of the rate equations for the free and donor-bound electron densities are obtained. We show that the self-oscillations in both free and donor-bound electron densities are an intrinsic feature of the photoinduced breakdown phenomenon. Good agreement is obtained by comparing the model calculations of the self-oscillations in the electron densities with those observed experimentally. Our model also provides an estimate of the semiconductor parameter ranges, namely the donor concentration, electron-hole recombination rates, and lattice temperature in which self-oscillations are predicted.

The paper is laid out as follows: In Sec. II, the experimental setup, the samples used, and the experimental results are presented. A model for the photoinduced donor breakdown and an analysis of the resulting steady state as well as dynamics of the free and donor-bound electron densities are detailed in Sec. III. A discussion and comparison of the model with the experimental results are given in Sec. IV. An analysis that determines the conditions on the model parameters for which the self-oscillations are expected is presented in the Appendix.

II. EXPERIMENTAL PROCEDURE AND RESULTS

We investigated several samples of nominally undoped, semi-insulating bulk GaAs, grown by the liquid-encapsulated Czochralski (LEC) technique. The samples, with dimensions of $4\times6\times0.5$ mm^3, were cut from different wafers (that are used as substrates for quantum structure growth). Electron heating is achieved by microwave irradiation (instead of the commonly used direct electric field). Using microwaves allows us to apply an electric field in a contactless manner, whereby we obtain a macroscopically uniform electric-field distribution within the sample. The samples are placed in the antinode of the microwave electric field in an 8-mm waveguide which is short circuited at one end. The waveguide was immersed in liquid He or in cold He gas so that the temperature was varied in the range of $T=2-30$ K. Laser light (He-Ne and tunable Ti-Al_2O_3 lasers as well as a quartz-halogen filament lamp were used) illuminated the sample through a pinhole in the waveguide. This excitation was modulated at a frequency varying in the range of 10–400 Hz.

A stabilized 36-GHz Gunn diode was used as the MW source. An electrically controlled attenuator allowed us to vary the incident MW power continuously so that the power incident on the sample was in the range of 0.1–20 mW. The reflected MW radiation was directed onto a diode detector by a circulator.

The reflected microwave power was modulated by the photoexcitation of the sample. This modulation signal is proportional to the microwave power absorbed by the photoexcited free electrons. The photoinduced microwave absorption (PMA) is $\sim\sigma\varepsilon^2\sim\sigma P$, where σ is the conductivity, and ε and P are the microwave field strength and microwave power, respectively. The conductivity at the MW frequency ω is given by $\sigma=\sigma_0/(1+\omega^2\tau^2)$, where $\sigma_0=en\mu$ is the dc conductivity, $\tau=\mu m^*/e$ is the momentum relaxation time of the free electrons, and m^* is the electron effective mass. At low temperatures ($T<30$ K) the dc mobility of LEC-grown GaAs is of the order of $\mu\sim10^4-10^5$ cm^{2}V^{-1}s^{-1}.[22] Hence $\omega\tau\ll1$ and PMA $\sim\sigma_0P=en\mu P$. Therefore, the PMA signal is proportional to the free-electron concentration.

We studied the steady-state and temporal dependences of PMA on the MW power and on the photoexcitation intensity (I_L). Similarly, the PL and PMA spectral dependences on these parameters were also studied. The PL and the signal from the MW diode detector were analyzed by a lock-in amplifier or by an oscilloscope that has a fast Fourier transform function.

Figure 1(a) shows the PMA dependence on P for $I_L=1$ mW/cm^2. At a certain threshold MW power, an abrupt increase of the PMA is observed. Then a hysteresis behavior occurs as the MW power sweep direction is reversed. The threshold MW power depends weakly on the light-excitation intensity (in the range of $I_L=0.1-30$ mW/cm^2). The threshold decrease of the PL intensity at an energy of 1.49 eV for the same MW power [Fig. 1(b)] will be discussed below.

Under cw microwave and light irradiation conditions, the PMA signal starts to oscillate when P exceeds the threshold value (Figs. 2 and 3). The frequency of the self-oscillations depends on both P and I_L, as can be seen from the Fourier transforms shown in Fig. 4.

The free-electron lifetime was extracted from the tem-

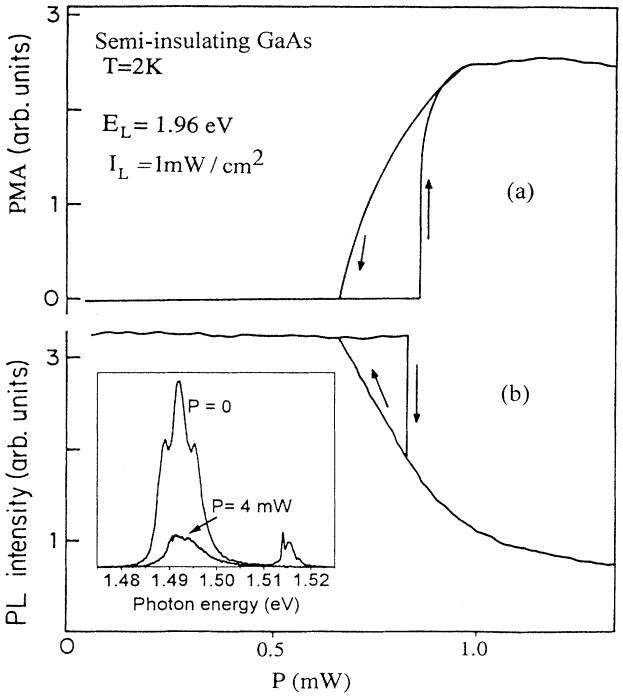

FIG. 1. (a) The photoinduced microwave absorption (PMA) dependence on incident MW power. (b) Similarly for the photoluminescence intensity monitored at 1.49 eV. Inset: the photoluminescence spectra observed without microwave irradiation and at P higher than the breakdown threshold.

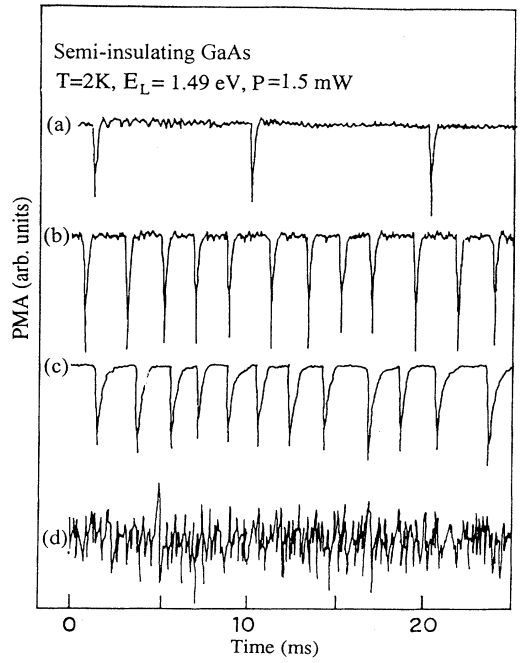

FIG. 2. Self-oscillations of the photoinduced microwave absorption (PMA). The light intensity values I_L are (a) 0.6, (b) 2, (c) 6, and (d) 20 mW/cm^{-2}.

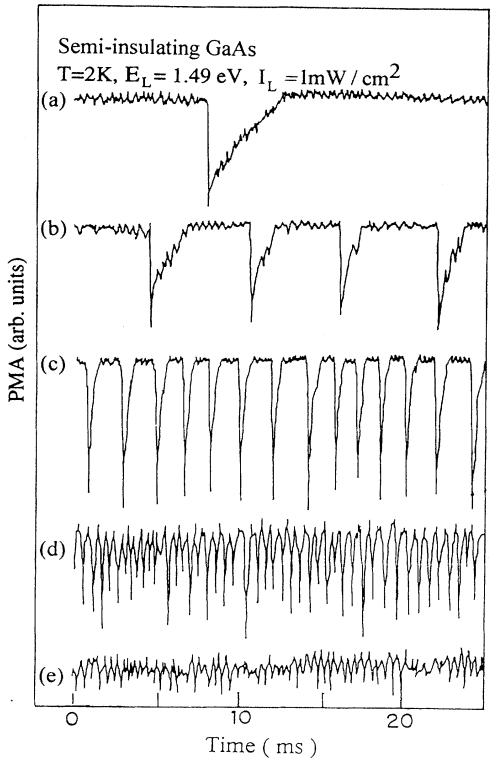

FIG. 3. Similar to Fig. 2 for the incident MW power values P: (a) 1, (b) 1.5, (c) 3.5, (d) 8, and (e) 18 mW.

poral response of the PMA signal to a square-shaped modulated photoexcitation. The PMA decays exponentially under very low MW power irradiation, with a time constant $t_R \approx 0.3$ ms.

Photoluminescence spectra observed with and without MW irradiation are shown in the inset of Fig. 1. The

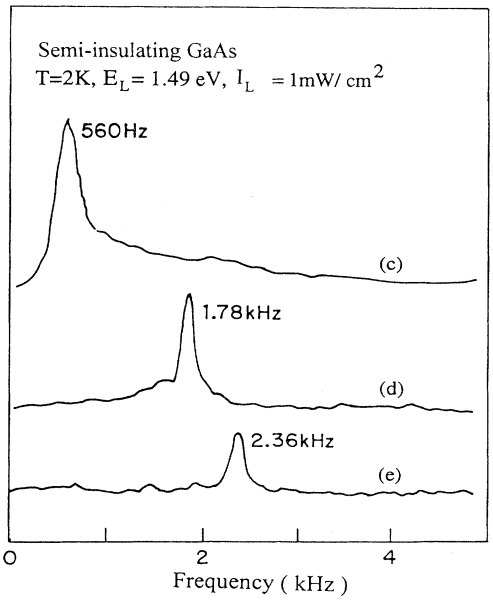

FIG. 4. Fourier transforms of the three PMA wave forms (c), (d), and (e) shown in Fig. 3.

low-energy PL band (around 1.49 eV) is due to donor-acceptor-pair (DAP) recombination, and the PL band near 1.51 eV is due to bound exciton recombination.[22] The low-temperature intensity ratio between these two bands provides a rough estimate of the impurity concentration. Similar PL spectra were reported for undoped GaAs samples with shallow donor concentrations estimated to be about $(2-5)\times 10^{14}$ cm^{-3}.[23]

The PL intensity decreases when the MW power P exceeds the same threshold as that required to cause the abrupt increase in the PMA [Fig. 1(b)]. This decrease is observed for all PL bands. A hysteresis loop is observed, similar to that of the PMA.

The PMA nonlinear behavior and its self-oscillations are also observed at photoexcitation energies lower than the band-gap energy. Figure 5 shows the PMA excitation spectrum observed at low microwave power (P=0.1 mW). The appearance of the PMA for an excitation energy as low as 0.8 eV is attributed to an electron excitation from the EL2 state [which is associated with the double As (Ga) antisite defect[24]] to the conduction band. The band at $\sim$1.50 eV is associated with an electron transition from acceptor levels to the conduction band. The sharp decrease of the PMA at photoexcitation energies near and above E_{gap} is due to the strong surface recombination of the electron-hole pairs. It should be noted that there are some differences between the results of this work and our preliminary report.[17] These are due to a difference in the sample structure (there we studied samples with thin epilayers of pure GaAs).

We studied the effect of increasing the ambient temperature on the observed PMA nonlinearities. The PMA self-oscillations and the threshold dependence in the PMA and the PL disappeared at temperatures above 10 K.

Self-oscillations of the PMA were not observed in other GaAs samples with higher impurity concentrations, for which exciton emission was not observed.

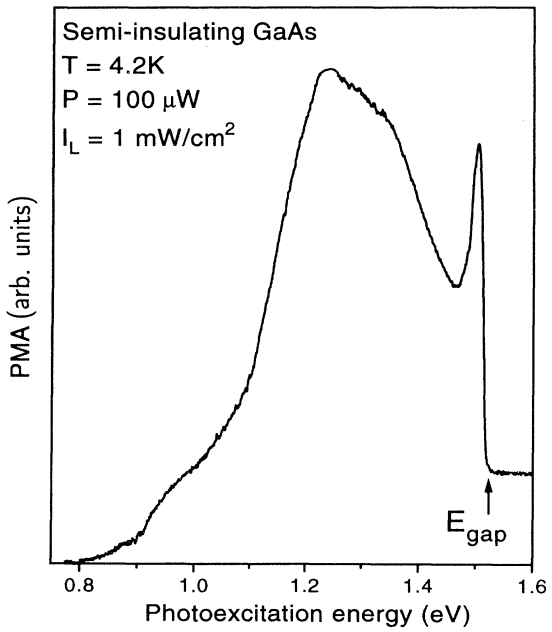

FIG. 5. The photoinduced microwave absorption (PMA) excitation spectrum observed at low microwave power.

III. MODEL AND ANALYSIS

We consider a highly compensated semiconductor with one type of donor and acceptor (Fig. 6). In the dark, the donors are completely ionized and the acceptors are occupied by electrons. Photoexcitation generates electrons in the conduction band at a rate of G (with partial neutralization of the donors). Only free electrons will be considered, since the holes are rapidly trapped by charged acceptors and, therefore, the hole concentration is small in comparison with that of the free electrons.[25] The applied electric field ε heats up the free electrons, which in turn impact ionize the bound electrons in the 1s donor level. In this analysis, the electrons are assumed to be heated by either a microwave or a dc electric field.[26] Then the rate equations for the free-electron density $n(t)$ and for the donor-bound electron density $m(t)$ are

$$\frac{dn}{dt}=G+\beta nm-\gamma n(N_D-m)-\frac{n}{\tau_1}+\gamma mN_{ct}\ , \quad \text{(1a)}$$

$$\frac{dm}{dt}=\gamma n(N_D-m)-\beta nm-\frac{m}{\tau_2}-\gamma mN_{ct}\ . \quad \text{(1b)}$$

Here $\gamma n(N_D-m)$ is the rate of free-electron capture by the ionized donors, N_D is the donor density, and γ is the capture rate coefficient. The recombination rates of free and donor-bound electrons with holes (mainly bound to acceptors) are given by the terms n/τ_1 and m/τ_2, where τ_1 and τ_2 are the respective recombination times. The term γmN_{ct} describes the thermal excitation of electrons from the donor levels to the conduction band. $N_{ct}=N_c\exp(-E_i/kT)$, where N_c is the density of

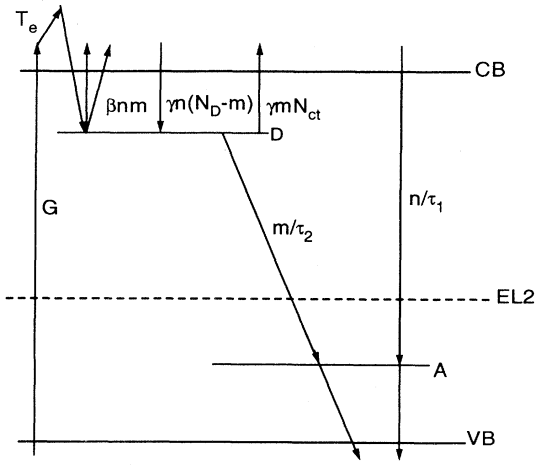

FIG. 6. Energy-level scheme and dynamic processes of the model used to analyze the nonlinear behavior of the free and donor-bound electron density (n and m, respectively).

conduction-band states, E_i is the ionization energy of donors, and T is the lattice temperature. The term βnm describes the impact-ionization rate of neutral donors by hot electrons, where β is the impact-ionization coefficient.

In general, the coefficients γ, τ_1, τ_2, and β depend on the hot-electron energy (E_e). We assume that the main effect of the hot electrons is due to the dependence of β on E_e. Hence, following Refs. 6 and 9, we neglect the dependence of γ, τ_1, and τ_2 on E_e. Under electron heating there are variations in the free-electron-energy-distribution function, and the mean value of E_e increases with increasing ε. We thus have to determine the dependence of β on ε. If the hot electrons have a Maxwellian distribution function with an effective electron temperature $T_e=2E_e/3k$, then β may be approximated by $\beta=\beta_0\exp(-E_i/kT_e)$, where $\beta_0=\pi a_b^2 v_e$, a_b is the donor Bohr radius, and v_e is the electron velocity.[27] Then, the electron temperature dependence on ε can be found from the following balance equation:[9,26]

$$\frac{dT_e}{dt}=\frac{2}{3k}e\mu(T_e,n)\varepsilon^2-\frac{T_e-T}{\tau_e(T_e,n)} . \tag{2}$$

The first term on the right-hand side describes the heating of free electrons by the applied electric field ε, and the second term describes the hot-electron cooling. τ_e is the energy-relaxation time. Since the electron-energy-relaxation rate is much larger than the rate of electron-density variation, we can approximate the electron temperature by the value obtained from the steady-state solution $dT_e/dt=0$:

$$T_e(n,\varepsilon)=T+\frac{2e}{3k}\tau_e(T_e,n)\mu(T_e,n)\varepsilon^2 . \tag{3}$$

In order to solve Eq. (3) for T_e, it is necessary to determine the dependencies $\mu(T_e,n)$ and $\tau_e(T_e,n)$. In LEC-grown GaAs crystals with impurity concentrations of about $10^{14}-10^{15}$ cm^{-3}, the electron mobility at temperatures $T<30$ K is determined by ionized-impurity scattering,[22] and, therefore, $\mu\propto T_e^{3/2}$. At $T_e<50$ K the electron-energy losses are due to their interaction with acoustic phonons and to impact ionization of impurities.[27] In GaAs, the electron-phonon interaction is primarily via the piezoelectric potential with an energy-relaxation time $\tau_e\propto T_e^{1/2}$. Substituting these temperature dependencies of μ and τ_e into Eq. (3) results in the so-called runaway effect: an electron heating rate [first term in Eq. (2)] increases with ε faster than the energy-loss rate to the phonons.[9,21] Impact-ionization losses can limit this effect and the dependence $T(\varepsilon)$ will then show an S-type behavior. Therefore the electron temperature increases sharply at a certain ε, and can induce the impurity breakdown.[21] The solution of the nonlinear Eq. (3) depends very strongly on the values of the parameters μ and τ_e and, implicitly, on N_D. Therefore, the dependence $T_e(n,\varepsilon)$ cannot be determined explicitly. Moreover, it is necessary to take into account the dependence of the electron mobility on the free-electron density. Various mechanisms leading to a $\mu(n)$ dependence were discussed in Refs. 8 and 9 in connection with S-shaped current-voltage curves in the case of impurity breakdown. One of these mechanisms is the following: with increasing free-electron density there is an increased screening of the charged-impurity electric field, and this results in a decrease in the electron-ionized impurity scattering rate.

We tried to overcome these difficulties by phenomenologically taking into account the runaway effect and the increased screening of the random electric field of the charged impurities. We assume a linear dependence of the electron temperature T_e on the electron density, and a quadratic one on the electric field ε ($T_e\propto n\varepsilon^2$) for the following reasons. First, a numerical estimate of the mobility increase with increasing n shows that a linear approximation of the Brooks-Herring expression for electron-ionized impurity scattering[26] is reasonable in the free-electron density range of $10^{11}-10^{13}$ cm^{-3}. Second, the runaway effect can also be qualitatively described by this dependence. For an electric field lower than the breakdown value, the free-electron density is low and there are few high-energy runaway electrons that can produce an impact ionization. With increasing electron density due to an impact ionization, the increased electron-electron-scattering rate [which becomes significant for $n>10^{11}$ cm^{-3} (Ref. 28)] redistributes the energy of the overheated electrons among all the free electrons, and this results in an increase of the mean electron energy. Hence we assume a linear increase of the effective electron temperature T_e as the electron density increases. Using Eq. (3), we introduce both these processes in our model by setting the impact-ionization coefficient as

$$\beta=\beta_0\exp\left[-\frac{E_i}{kT_e}\right]=\beta_0\exp\left\{-\frac{1}{(1+\lambda n)P_1}\right\} , \tag{4}$$

with

$$P_1=\tfrac{2}{3}\mu_0 e\tau_e\varepsilon^2/E_i . \tag{5}$$

P_1 is a dimensionless control parameter that measures the absorbed electric power per electron in units of E_i/τ_e. It is defined for a constant μ_0, the electron mobility in the absence of a large free-electron density. To a first approximation, P_1 is independent of the electron density. λ is a constant to be determined by fitting this model to the self-oscillation periods.

It should be noted that the impact-ionization coefficient dependence on the free-electron density was previously considered[9,29] within the framework of the free-electron screening of ionized donors. In Ref. 29 the dependence was assumed to be $\beta=\beta_0\exp(-E_i/kT_e)+zn$ (where T_e does not depend on n, and z is a constant), and it leads to nonlinear effects. Although this choice was convenient for the numerical simulations, it was not supported by any physical arguments.

We rewrite now Eqs. 1(a) and 1(b) using the dimensionless units $x=\gamma\tau_2 m$, $y=\gamma\tau_2 n$, $N=\gamma\tau_2 N_D$, $C=\gamma\tau_2 N_{ct}$, $g=\gamma\tau_2^2 G$, $r=\tau_2/\tau_1$, $\tau=t/\tau_2$, $R=\beta/\gamma$, $R_0=\beta_0/\gamma$, and $\lambda_1=\lambda/\gamma\tau_2$:

$$\frac{dy}{d\tau} = g + yx(R+1) - y(N+r) + Cx \ , \tag{6a}$$

$$\frac{dx}{d\tau} = yN - yx(R+1) - x(1+C) \ . \tag{6b}$$

These equations, describing the photoinduced impurity breakdown, are very similar to those obtained for exciton breakdown where the linear dependence $T_e(n)$ was associated with the effect of electron-hole scattering on the electron-energy gain in a microwave field ($\omega\tau \gg 1$).[12]

The analytical dependencies of the steady-state solution y_0 (and also x_0) on the control parameters (g and P_1) are obtained from[6]

$$g = \frac{y_0 N}{y_0(R+1)+C+1} + y_0 r \ , \tag{7a}$$

$$P_1 = \left[(1+\lambda_1 y_0) \ln \left\{ \left[\frac{1}{R_0} \left[\frac{N}{g - y_0} r - \frac{1+y_0+C}{y_0} \right] \right]^{-1} \right\} \right]^{-1} . \tag{7b}$$

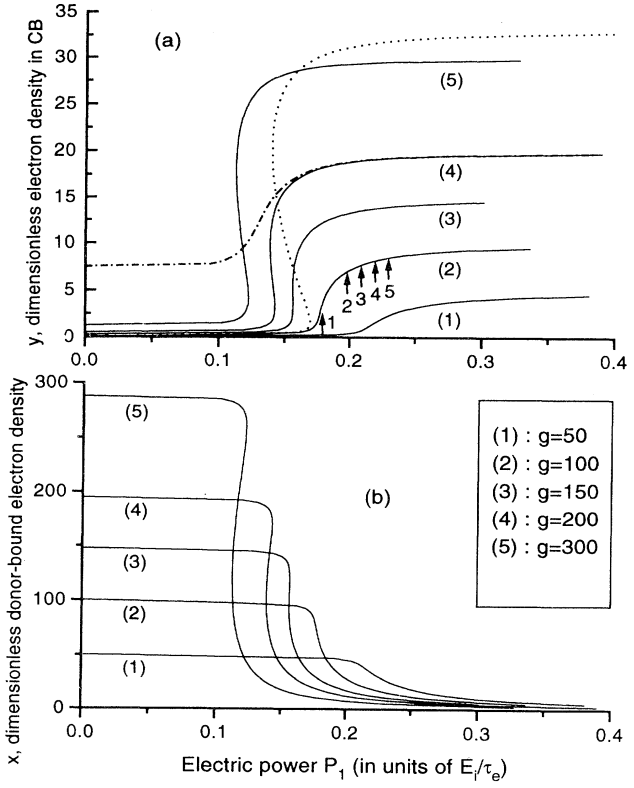

FIG. 7. (a) The calculated steady-state free-electron concentration as a function of the electric power (P_1) for various photoexcitation levels at $T=2$ K. The concentration is given in units of $y=\gamma\tau_2 n$ ($y=10$ corresponds to $n \approx 10^{13}$ cm^{-3} using the values of $\gamma=10^{-9}$ cm^3 s^{-1} and $\tau_2=10^{-3}$ s). (b) Similar for the donor-bound electron density in units of $x=\gamma\tau_2 m$. Dimensionless model parameters: $\gamma\tau_2 N_D=500$, $\beta_0/\gamma=1000$, $\tau_2/\tau_1=10$, and $\lambda_1=0.03$. The dotted curve in the upper part corresponds to $g=100$ and $r=4$. The dotted-dashed curve corresponds to $T=10$ K. The arrows indicate the unstable states for which temporal simulations are shown in Fig. 10.

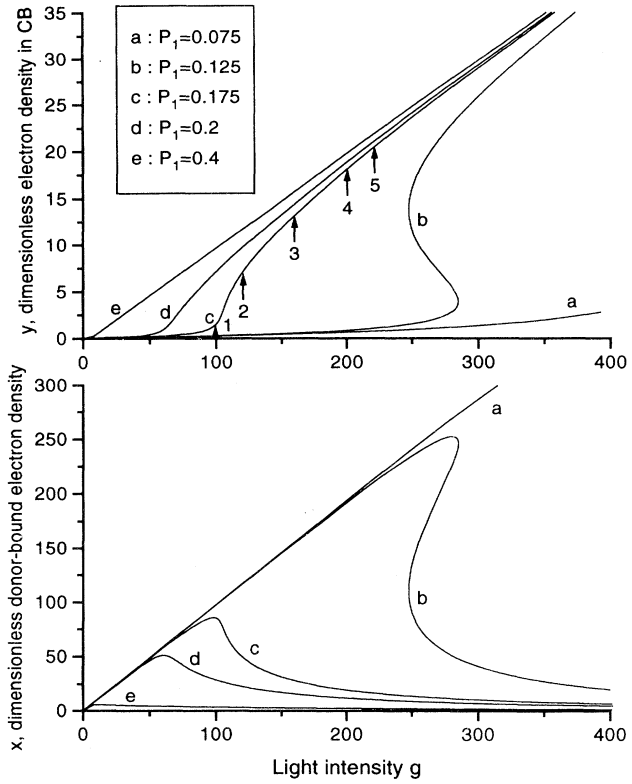

FIG. 8. The calculated steady-state dependencies of the free and donor-bound electron densities as a function of the photoexcitation intensity for various electric power values (P_1). All parameters are the same as given in Fig. 7.

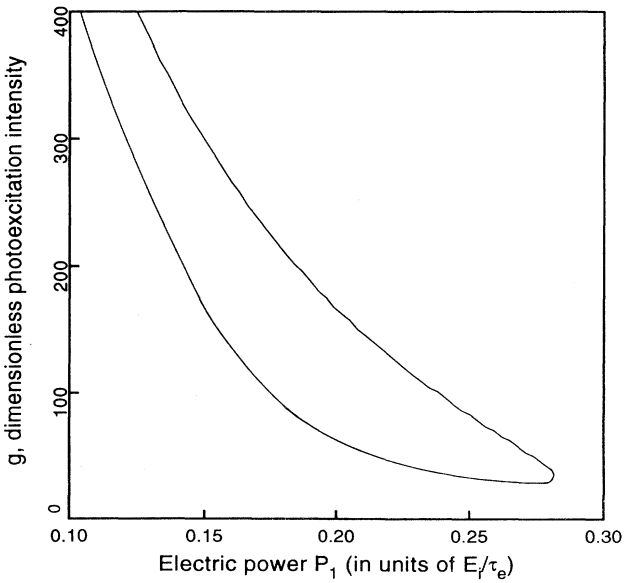

FIG. 9. The control parameter (light intensity g vs electric power P_1) plane. Inside the contour there are self-oscillations in the electron density. The dimensionless model parameters are the same as given in Fig. 7.

The calculated steady-state dependencies of the free and donor-bound electron densities on the incident electric power and on the photoexcitation intensity are shown in Figs. 7 and 8, respectively. An S-shaped curve and bistability are obtained for both the free and donor-bound electron densities in limited regions of the photoexcitation intensity and electric power. The model calculations show that the shape of the curves depends on $r(=\tau_2/\tau_1)$. As r increases, the S-shaped dependence vanishes. This demonstrates a transformation from a first-order phase transition to a second-order one in the electron density behavior,[6] as the ratio between the lifetimes τ_2 and τ_1 varies.

An analysis of the stability of the steady-state solutions shows that there is a range of control parameters (light intensity and electric field) wherein they are unstable. The analysis is given in the Appendix, and its results are presented in Fig. 9. The temporal behavior of the photoinduced breakdown reveals that self-oscillations in the free and donor-bound electron densities are obtained only for the control parameters that are inside the contour shown in Fig. 9. The numerical solutions of the dynamic equations [Eqs. (6a) and (6b)] for some values of the control parameters are shown in Fig. 10. In terms of the dimensionless parameters, the nonlinear effects occur in the following ranges: $\gamma\tau_2^2 G \approx 30-300$, $\gamma\tau_2 N_D \approx 100-1000$, $\tau_2/\tau_1 \approx 3-15$, $\beta_0/\gamma \approx 500-1500$, and $\lambda/\gamma\tau_2 \approx 0.01-0.1$. For the photoexcitation levels of $G=10^{17}-10^{18}$ photon/cm^3 s used in the experiments and for the shallow donor concentration range of $N_D=(2-5)\times 10^{14}$ cm^{-3} we obtain $\tau_2 \approx (0.3-3)\times 10^{-3}$ s and, hence, $\gamma \approx 10^{-9}$ cm^3 s^{-1} and $\beta_0 \approx 10^{-6}$ cm^3 s^{-1}. This choice of parameters yields a good agreement of the model with the experimental data, and is discussed in Sec. IV. Table I summarizes the model parameters and compares them to available values appearing in the literature.

Increasing the ambient temperature leads to a decreased population of donor-bound electrons, and the self-oscillations disappear. Indeed, our numerical solutions show that for $T > 10$ K the self-oscillations disappear (using the donor ionization energy of 5 meV).

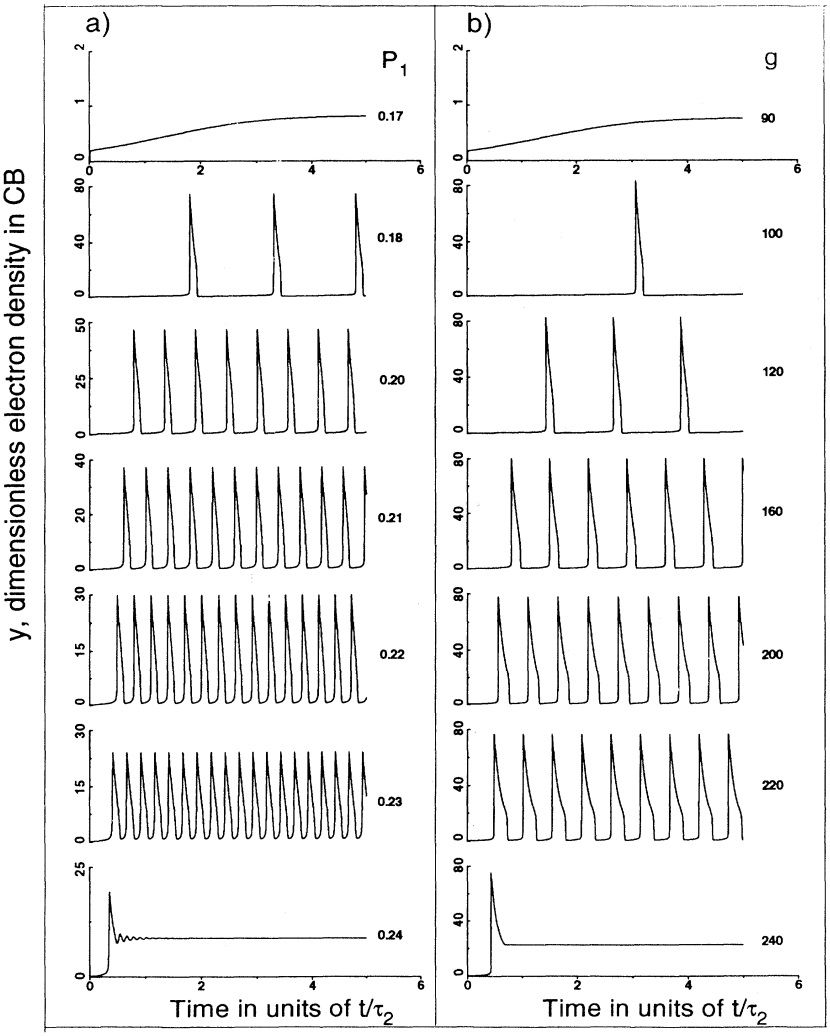

FIG. 10. Numerical simulations of the self-oscillations in the electron density under impurity breakdown. The dimensionless model parameters are the same as given in Fig. 7. (a) Various electric powers P_1 at $g=100$. (b) Various light intensities g at $P_1=0.175$.

TABLE I. Model parameters.

Parameter	This work	From references	
γ (cm^3 s^{-1})	$\sim 10^{-9}$	10^{-6}	4
		2×10^{-12}	11
β_0 (cm^3 s^{-1})	$\sim 10^{-6}$	2×10^{-8}	4
		$\approx 10^{-5}$	32
τ_2 (s)	$(0.3-3)\times10^{-3}$	$10^{-5}-10^{-4}$	25

IV. DISCUSSION AND CONCLUSIONS

We have shown that nonlinear effects due to impact ionization in semi-insulating GaAs at low temperatures can be explained by a one-level donor model, assuming that the electron temperature depends on the electron density. This dependence provides the simplest approximation to the complex hot-electron processes that take place in the low-temperature impurity breakdown in GaAs, and in particular the electron runaway effect. Indeed, the breakdown in GaAs starts at very low direct electric fields (on the order of 1 V/cm);[1,3,11] the equivalent threshold microwave electric field value ($\varepsilon\sim\sqrt{P}$) in our experiments is approximately the same. A simple estimate of the energy gained by a free electron in GaAs, moving over a distance equal to its mean free path at this field value, shows that the energy gained is insufficient to induce a breakdown of the donors. However, such a low threshold value can be easily understood by taking into account the electron runaway effect. It follows from Eq. (3) that an abrupt increase of T_e occurs at a rather low electric field when $T_e\sim 2$ T,[21] and this initiates the impurity breakdown. This means that the runaway effect is essential for breakdown in GaAs. Unfortunately, a microscopic theory of the impurity-breakdown phenomenon driven by the runaway effect is still unavailable. We suggest that the $T(n)$ dependence assumed in our model [Eq. (4)] takes the runaway effect into account since a good agreement between the experimental results and those calculated with our phenomenological model is obtained.

The model calculations yield the recombination time range wherein the self-oscillations are possible, namely $\tau_2\approx(0.3-3)\times10^{-3}$ s. The calculated self-oscillation period (Fig. 10) varies in the range of $(0.3-1)\times\tau_2$ and these give the estimate of the self-oscillation frequency. The latter agrees with the observed self-oscillation frequency range of 0.5–3 kHz. In addition, the self-oscillations are predicted for $\tau_2/\tau_1=3-15$. This leads to a calculated free-electron recombination time which is also in agreement with the experimental value $t_R\approx0.3$ ms.[30] Note that a recombination time (τ_2) of milliseconds is expected for remote donor-acceptor pairs under a very low excitation level.[25,31]

Our experiments under microwave irradiation and the model of the photoinduced impurity breakdown demonstrate that self-oscillations in both free and donor-bound electron densities are an intrinsic feature of the photoinduced breakdown phenomenon. Self-oscillations occur even when there is no S-shaped electron-density dependence on the electric field. The model shows that as $r=\tau_2/\tau_1$ increases, the S-shape dependence disappears but instabilities persist. For $r<1$, there are no self-oscillations and the steady-state solutions are stable.

A self-oscillation behavior is possible only when the system exhibits both positive and negative feedbacks. In our model, impact ionization of the donor level is a positive feedback, and the free-electron–acceptor recombination and donor-acceptor transitions are negative feedbacks. The impact-ionization rate coefficient β must increase with increasing free-electron density for self-oscillations to occur.

In summary, we observe a threshold increase in the photoinduced microwave absorption and a concurrent decrease of the donor-acceptor pair photoluminescence in semi-insulating bulk GaAs for temperatures below 10 K. Self-oscillations in the PMA are observed when the incident MW power exceeds a threshold value. The frequency of the self-oscillations increases with increasing light intensity and the incident MW power, and is in the range of 0.5–3 kHz. The self-oscillations occur in a limited range of MW power and photoexcitation level. All these features are predicted by the one-level photoinduced impurity-breakdown model which takes into consideration both free-electron and donor-acceptor pair recombination. In both the model and the experiment, the self-oscillations occur under spatially homogeneous distribution of the electric (microwave) field. The characteristic time of DAP recombination controls the self-oscillation frequency.

ACKNOWLEDGMENTS

The research at Technion was done in the Barbara and Norman Seiden Center for Advanced Optoelectronics. B.M.A. acknowledges the support of Foundation Rich (France) and Alexander Goldberg Fund of the Technion.

APPENDIX

In order to find the conditions that the model parameters must satisfy so that self-oscillations of the electronic densities will occur, we analyzed the local temporal stability of a solution of Eqs. (1) in the vicinity of the steady states. If the steady state (n_0,m_0) is an unstable focus, a self-oscillation regime of the dynamic solutions can arise and, similarly to Ref. 12, this leads to the following conditions on the parameters:

(1) $r=\dfrac{\tau_2}{\tau_1}>1$,

(2) $A_{11}>1$,

(3) $\sqrt{\gamma\tau_2(\tau_2/\tau_1-1)(n_0\beta/\gamma+n_0+N_{ct})}>(A_{11}+1)/2$,

where

$$A_{11}=\gamma\tau_2\left\{\left[\frac{3\beta\lambda\tau_2 n_0 E_i}{2\mu_0 e\tau_e\varepsilon^2(1+\lambda_{n_0})^2}+\frac{\beta}{\gamma}+1\right]\times\left[G\tau_2-n_0\frac{\tau_2}{\tau_1}\right]-n_0\left[\frac{\beta}{\gamma}+1\right]-N_D-N_{ct}\right\}-\frac{\tau_2}{\tau_1}\ .$$

Since n_0 and β are functions of G and P [determined by Eqs. (4) and 7(a)], it is possible to find analytically the range of control parameters (light intensity and electric field) wherein the stationary value of electron density is unstable (it was calculated and is presented in Fig. 9). Numerical solutions of the dynamic Eqs. (6) in this range of the parameters are shown in Fig. 10.

[1]K. Aoki, T. Kobayashi, and K. Yamamoto, J. Phys. Soc. Jpn. **51**, 2373 (1982).

[2]S. W. Teitsworth, R. M. Westervelt, and E. E. Haller, Phys. Rev. Lett. **51**, 825 (1983).

[3]J. Spangler, U. Margull, and W. Prettl, Phys. Rev. B **45**, 12 137 (1992).

[4]E. Schöll, Appl. Phys. **48**, 95 (1989).

[5]U. Rau, W. Clauss, A. Kittel, M. Lehr, M. Bayerbach, J. Parisi, J. Peinke, and R. P. Huebener, Phys. Rev. B **43**, 2255 (1991).

[6]E. Schöll, in *Handbook on Semiconductors,* edited by T. S. Moss and P. T. Landsberg (North-Holland, Amsterdam, 1992), Chap. 8.

[7]A. L. McWhorter and R. H. Rediker, Proc. IEEE **47**, 1207 (1959).

[8]R. P. Khosla, J. R. Fisher, and B. C. Burkey, Phys. Rev. B **7**, 2551 (1973).

[9]R. Crandall, Phys. Rev. B **1**, 730 , 1970.

[10]S. M. Ryvkin, V. P. Dobrego, B. M. Konovalenko, and I. D. Yaroshetsky, Fiz. Tverd. Tela (Leningrad) **4**, 379 (1964).

[11]F. Karel, J. Oswald, J. Pastrnak, and O. Petricek, Semicond. Sci. Technol. **7**, 203 (1992).

[12]B. M. Ashkinadze and A. V. Subashiev, Pis'ma Zh. Eksp. Teor. Fiz. **46**, 284 (1987) [JETP Lett. **46**, 357 (1987)].

[13]A. F. Volkov and Sh. M. Kogan, Usp. Fiz. Nauk **96**, 633 (1968) [Sov. Phys. Usp. **11**, 881 (1969)].

[14]R. Romestain and C. Weisbuch, Phys. Rev. Lett. **45**, 2067 (1980).

[15]A. A. Manenkov, V. A. Milyaev, G. N. Mikhailova, and S. P. Smolin, Pis'ma Zh. Eksp. Teor. Fiz. **16**, 454 (1972) [JETP Lett. **16**, 322 (1972)].

[16]W. M. Chen, B. Monemar, E. Sorman, P. O. Holtz, M. Sundardam, J. L. Merz, and A. C. Gossard, Semicond. Sci. Technol. **7**, B253 (1992).

[17]B. M. Ashkinadze, E. Cohen, Arza Ron, and L. N. Pfeiffer, Semicond. Sci. Technol. **9**, 570 (1994).

[18]A. Kastalskii, Phys. Status Solid A **15**, 599 (1973).

[19]W. Quade, G. Hüpper, E. Schöll, and T. Kuhn, Phys. Rev. B **49**, 13 408 (1994).

[20]B. Kehrer, Q. Quade, and E. Schöll, in *Proceedings of the 22nd International Conference on the Physics of Semiconductors, Vancouver, 1994,* edited by D. J. Lockwood (World Scientific, Singapore, 1995).

[21]I. B. Levinson, Fiz. Tverd. Tela (Leningrad) **7**, 1362 (1965) [Sov. Phys. Solid State **7**, 1098 (1965)].

[22]M. Maciaszek, D. M. Rogers, R. P. Bult, T. Steiner, Yu Zhang, S. Charbonneau, and M. L. W. Thewalt, Can. J. Phys. **67**, 384 (1989).

[23]W. M. Duncan and G. H. Westphal, in *GaAs and Related Compounds,* edited by W. T. Lindley, IOP Conf. Proc. No. 83 (Institute of Physics and Physical Society, London, 1986), p. 39.

[24]P. W. Yu, Appl. Phys. Lett. **44**, 330 (1984).

[25]D. Bimberg, H. Münzel, A. Steckenborn, and J. Christen, Phys. Rev. B **31**, 7788 (1985).

[26]E. M. Conwell, *High Field Transport in Semiconductors,* edited by F. Seitz, D. Turnbull, and H. Ehrenreich, Solid State Physics Suppl. No. 9 (Academic, New York, 1967).

[27]R. Ulbrich, Phys. Rev. B **8**, 5719 (1973).

[28]T. Kurosawa, J. Phys. Soc. Jpn. **20**, 1405 (1965).

[29]K. Aoki, N. Mugibayashi, and K. Yamamoto, Phys. Scr. **T14**, 76 (1986).

[30]A. Akimov, V. Krivolapchuk, N. Poletaev, and V. Shofman, Fiz. Tekh. Poluprovodn. **27**, 314 (1993) [Sov. Phys. Semicond. **27**, 171 (1993)].

[31]J. M. Chamberlain and R. A. Stradling, Solid State Commun. **7**, 1275 (1969).

[32]This value is estimated for $a_B \approx 100$ Å and $v_e \approx 3 \times 10^6$ cm/s.